

# IDCS J1426.5+3508: COSMOLOGICAL IMPLICATIONS OF A MASSIVE, STRONG LENSING CLUSTER AT $Z = 1.75$

ANTHONY H. GONZALEZ<sup>1</sup>, S. A. STANFORD<sup>2,3</sup>, MARK BRODWIN<sup>4,5</sup>, COSIMO FEDELI<sup>1</sup>,  
ARJUN DEY<sup>6</sup>, PETER R. M. EISENHARDT<sup>7</sup>, CONOR MANCONE<sup>1</sup>, DANIEL STERN<sup>7</sup>, GREG ZEIMANN<sup>2</sup>

*Accepted to The Astrophysical Journal*

## ABSTRACT

The galaxy cluster IDCS J1426.5+3508 at  $z = 1.75$  is the most massive galaxy cluster yet discovered at  $z > 1.4$  and the first cluster at this epoch for which the Sunyaev-Zel'Dovich effect has been observed. In this paper we report on the discovery with *HST* imaging of a giant arc associated with this cluster. The curvature of the arc suggests that the lensing mass is nearly coincident with the brightest cluster galaxy, and the color is consistent with the arc being a star-forming galaxy. We compare the constraint on  $M_{200}$  based upon strong lensing with Sunyaev-Zel'Dovich results, finding that the two are consistent if the redshift of the arc is  $z \gtrsim 3$ . Finally, we explore the cosmological implications of this system, considering the likelihood of the existence of a strongly lensing galaxy cluster at this epoch in a  $\Lambda$ CDM universe. While the existence of the cluster itself can potentially be accommodated if one considers the entire volume covered at this redshift by all current high-redshift cluster surveys, the existence of this strongly lensed galaxy greatly exacerbates the long-standing giant arc problem. For standard  $\Lambda$ CDM structure formation and observed background field galaxy counts this lens system *should not exist*. Specifically, there should be *no* giant arcs in the entire sky as bright in F814W as the observed arc for clusters at  $z \geq 1.75$ , and only  $\sim 0.3$  as bright in F160W as the observed arc. If we relax the redshift constraint to consider all clusters at  $z \geq 1.5$ , the expected number of giant arcs rises to  $\sim 15$  in F160W, but the number of giant arcs of this brightness in F814W remains zero. These arc statistic results are independent of the mass of IDCS J1426.5+3508. We consider possible explanations for this discrepancy.

*Subject headings:* galaxies: clusters: IDCS J1426.5+3508 – gravitational lensing: strong – cosmology: observations, cosmological parameters

## 1. INTRODUCTION

Galaxy clusters have historically played a central role in cosmology, with the most massive and distant systems providing the most profound insights. For example, observations of the Coma cluster provided the first evidence for dark matter (Zwicky 1933), while the existence of exceptionally massive clusters at early times was an important argument for  $\Omega_0 < 1$  (e.g., Carlberg et al. 1996; Donahue et al. 1998, and references therein). In recent years much attention has been given to the question of whether the most distant, highest mass clusters are consistent with a standard Gaussian  $\Lambda$ CDM cosmology, or whether one must invoke non-Gaussianity of the initial density fluctuations from inflation that seed structure formation. While these analyses have yielded divergent results (Hoyle et al. 2011; Enqvist et al. 2011; Cayón et al. 2011; Williamson et al. 2011), it is clear that the most massive, distant clusters remain valuable cosmological probes.

The galaxy cluster that is the focus of this paper was detected as part of the IRAC Distant Cluster Survey (IDCS), an ongoing 8.82 deg<sup>2</sup> survey within the *Spitzer* Deep, Wide-Field Survey (SDWFS Ashby et al. 2009) region that employs full photometric redshift probability distributions for a

4.5 $\mu$ m-selected galaxy catalog to identify galaxy clusters at  $0 < z < 2$ . This program extends the IRAC Shallow Cluster Survey (ISCS; Eisenhardt et al. 2008), which has yielded the largest sample of spectroscopically confirmed clusters at  $1 < z < 1.5$  by pushing both to lower mass and higher redshift. The cluster IDCS J1426.5+3508 was identified as a strong candidate for a high mass,  $z > 1.5$  cluster in this program and targeted for detailed follow-up. Spectroscopic observations with the *HST* WFC3 grism and LRIS on Keck, described in detail in Stanford et al. (2012), confirm that this cluster lies at  $z = 1.75$ .

While the existence of a cluster at this redshift is not surprising, multiple lines of evidence now suggest that this is a truly massive cluster. Stanford et al. (2012) report a *Chandra* X-ray mass estimate of  $M_{200} \approx 5.6 \times 10^{14} M_\odot$ , while Sunyaev-Zel'Dovich imaging from Brodwin et al. (2012) implies that the mass contained within a region overdense by a factor of 500 relative to critical density is  $M_{500} = 2.6 \pm 0.7 \times 10^{14} M_\odot$ , ( $M_{200} \approx 4.2 \times 10^{14} M_\odot$  for a typical halo concentration). For comparison, this Sunyaev-Zel'Dovich mass is only  $\sim 40\%$  lower than that of XMMU J2235.3-2557 at  $z = 1.39$  (Mullis et al. 2005; Rosati et al. 2009), which is the only published cluster at  $z \gtrsim 1.2$  more massive than IDCS J1426.5+3508. Meanwhile, the one spectroscopically confirmed galaxy cluster at higher redshift ( $z = 2.07$ , Gobat et al. 2011) has an estimated total mass of  $5.3 - 8 \times 10^{13} M_\odot$  – a factor of five to ten lower than IDCS J1426.5+3508.

In this paper we focus upon the discovery of a giant arc associated with this cluster and the implications of its existence in the context of  $\Lambda$ CDM structure formation. The layout of this paper is as follows. In §2 and 3 we present the discovery and attempted spectroscopy of the giant arc. In §4 we derive strong lensing constraints on the cluster mass, and discuss the redshift regime over which these constraints are consis-

<sup>1</sup> Department of Astronomy, University of Florida, Gainesville, FL 32611-2055

<sup>2</sup> Department of Physics, University of California, One Shields Avenue, Davis, CA 95616

<sup>3</sup> Institute of Geophysics and Planetary Physics, Lawrence Livermore National Laboratory, Livermore, CA 94550

<sup>4</sup> Department of Physics and Astronomy, University of Missouri, 5110 Rockhill Road, Kansas City, MO, 64110

<sup>5</sup> Harvard-Smithsonian Center for Astrophysics, 60 Garden Street, Cambridge, MA 02138

<sup>6</sup> NOAO, 950 North Cherry Avenue, Tucson, AZ 85719

<sup>7</sup> Jet Propulsion Laboratory, California Institute of Technology, Pasadena, CA 91109

tent with the SZ mass. We then extend our discussion in §5 to consider the probability for the discovery of a giant arc associated with this cluster. Finally, in §6 we summarize our results and consider potential theoretical modifications that may resolve the arc statistic discrepancy. Throughout this paper we use cosmological parameters consistent with the seven year WMAP results ( $\Omega_\Lambda = 0.728$ ,  $H_0 = 70.4 \text{ km s}^{-1}$ ,  $\sigma_8 = 0.809$ ; Komatsu et al. 2011).

## 2. DETECTION OF A GIANT ARC

We obtained *HST* imaging with the Advanced Camera for Surveys (ACS; Ford et al. 2003) and Wide-Field Camera 3 (WFC3; Kimble et al. 2008) as part of Cycle 17 program 11663 (PI: Brodwin) between 08 July 2010 and 07 November 2010. The total exposure times in F814W and F160W were 4.5 ks and 2.6 ks, respectively. Further details are provided in Stanford et al. (2012). Subsequent grism observations in Cycle 18, coupled with Keck spectroscopy, confirm that the galaxy cluster is real and at  $z = 1.75$  (Stanford et al. 2012).

Within the *HST*/ACS and WFC3 imaging we identify a highly elongated object which we interpret as a strong arc lensed by the cluster. We present a composite F814W+F160W image of the cluster field in Fig. 1, highlighting this object. The length is  $4''.8$  but the width is unresolved in the *HST* photometry, and hence it easily satisfies the standard length-to-width criteria for a giant arc ( $l/w > 10$ ; Wu & Hammer 1993). The curvature of the object is consistent with lensing by the cluster potential, and the color can be used to further constrain the nature of the object.

### 2.1. Arc Photometry

We extract the magnitude of the arc within a polygonal aperture constructed to enclose the full extent of the arc. The enclosed area within the aperture is  $9.0 \text{ arcsec}^2$ , and the extent along the major axis is  $6''.7$  (Fig. 1). As part of this procedure we first use Source Extractor (Bertin & Arnouts 1996) to generate a background map. The flux and background are measured both within the source aperture and for an ensemble of blank-sky apertures surrounding the arc, from which we can calculate the aperture-to-aperture photometric variance. We measure  $F814W = 24.29 \pm 0.31 \text{ mag}$  and  $F160W = 23.75 \pm 0.21 \text{ mag}$  (AB). Given the large uncertainties in the total magnitude, the integrated color of the arc,  $F814W - F160W = 0.55 \pm 0.37 \text{ mag}$ , is only modestly constrained. To obtain an improved estimate of the color, we recompute the color within a smaller,  $0''.8 \times 0''.4$  rectangular aperture that includes the region with the highest signal-to-noise ratio (Fig. 1). Within this aperture we obtain a more precise, statistically consistent color,  $F814W - F160W = 0.25 \pm 0.13 \text{ mag}$ . As expected for an arc, we see no evidence for color changes along its length that might be indicative of a chance superposition of sources.

What does this color imply about the source galaxy? The fact that the source is not a drop-out in F814W constrains the redshift to be  $z \lesssim 6$ . The observed color is similar to that of  $z \sim 4$  *B*-band dropouts (Gonzalez et al. 2011). For a somewhat more complete picture of plausible redshifts, we consider the predicted colors from a suite of Bruzual & Charlot (2003) stellar population models. For a Chabrier (2003) mass function and solar metallicity, the observed color is inconsistent with passively evolving stellar populations at all redshifts. To be precise, single burst models in which star formation has ceased more than  $\sim 100 \text{ Myrs}$  earlier uniformly predict F814–F160W colors that are significantly redder than

observed regardless of the formation redshift. Conversely, models with an exponentially declining star-formation rate ( $\tau$ -models) can successfully reproduce the observed color at higher redshifts. These models place a lower bound on the redshift as a function of  $\tau$  and the assumed formation redshift. For  $\tau = 1 \text{ Gyr}$ ,  $1\sigma$  consistency with the observed color requires  $z > 1.75$  (2.5) for  $z_{\text{form}} > 2$  (3). Smaller values of  $\tau$  increase the minimum redshift.

### 2.2. Arc Geometry

The location of the arc is such that no nearby individual galaxies appear to be contributing significantly to the lensing, and the curvature is consistent with the centroid being nearly coincident with the brightest cluster galaxy (BCG). If we make the assumption that the lensing is indeed centered upon the BCG, then the radius of the arc is  $\theta = 14''.6 \pm 0''.2$ . There is however no guarantee that the BCG lies directly at the bottom of the potential in the absence of a detailed lensing model, so for the analysis below we assume an uncertainty of 30 kpc in the centroid, which corresponds to a  $3''.4$  uncertainty in the radius of the arc. For local clusters from the Lo-CuSS program roughly 68% of clusters have offsets between the BCG and X-ray peak less than this value (Sanderson et al. 2009).

## 3. GEMINI AND *HST* SPECTROSCOPY

We attempted to obtain a redshift for the giant arc using Gemini North. We targeted  $\text{Ly}\alpha$  emission during 6.5 hr of Director's Discretionary Time, using GMOS for long slit spectroscopy. The data were acquired between 26 June 2011 and 06 July 2011 (UT) using the B600 grism, which is blazed at  $4610 \text{ \AA}$ . We observed with a central wavelength of  $5150 \text{ \AA}$  and two pixel binning in both the spatial and spectral directions using a  $1''.0$  slit. The resultant spatial and spectral resolutions are  $0''.146 \text{ pix}^{-1}$  and  $0.9 \text{ \AA pix}^{-1}$ , respectively, and the slit was positioned to lie along the long axis of the arc at a position angle of  $270.85$  degrees. We obtained  $13 \times 1780 \text{ s}$  exposures, dithered in both the spatial and the spectral dimensions, for a total on-source exposure time of 6.43 hr. The seeing during these observations ranged from  $0''.67$  to  $1''.08$ , with a median seeing of  $0''.77$  based on an early M-type star which was serendipitously observed in the majority of the observations. Conditions during the observations were mostly photometric, but included some data taken during 70th percentile (patchy cloud) conditions.

The redshift constraints arising from the cluster redshift (i.e.,  $z > 1.75$ ) and the fact that the arc is detected in the F814W imaging (i.e.,  $z \lesssim 6$ ) provide a first bound on the redshift. Within this range we focused upon  $z \lesssim 4$  and designed the observations to be sensitive to strong  $\text{Ly}\alpha$  emission (comparable to a Lyman Alpha Emitter), if present for  $2 \lesssim z \lesssim 4$ . We reduced the data using standard long slit procedures within IRAF. Unfortunately, we detect neither any continuum nor any emission lines at  $3590 \text{ \AA} < \lambda < 6660 \text{ \AA}$  ( $2.0 < z < 4.5$  for  $\text{Ly}\alpha$ ).

We also attempted to obtain a redshift for the arc using *HST*/WFC3 grism data from program 12203 (PI Stanford). The data and reduction procedure are both described in Stanford et al. (2012). Neither continuum nor emission lines for the arc were detected with either the G102 or G141 grisms, which together cover the wavelength range  $0.8\mu\text{m} < z < 1.65\mu\text{m}$ . Using simulations run with the aXeSIM software, we calculate that the corresponding emission line detection threshold corresponds to  $f < 4 \times 10^{-16} \text{ erg s}^{-1} \text{ cm}^{-2}$

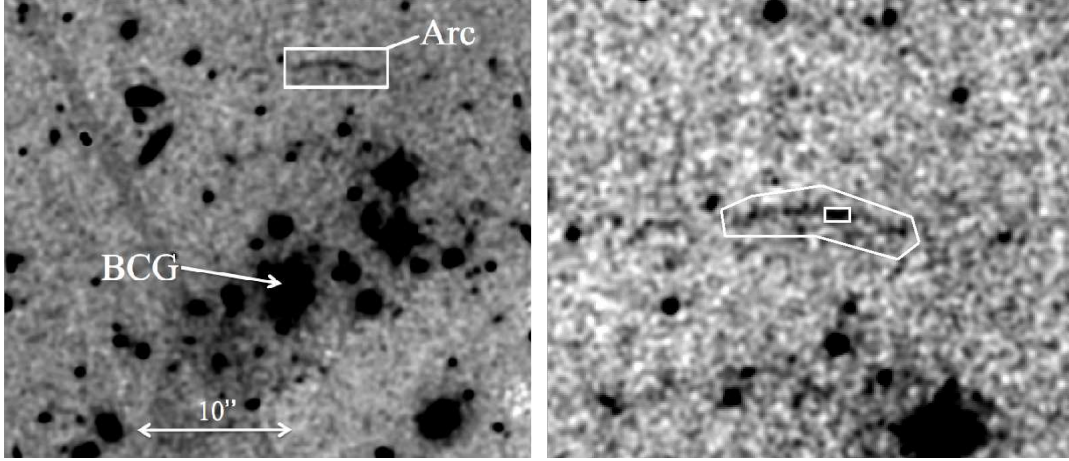


FIG. 1.— *Left*— Combined F814W+F160W image of the cluster center and giant arc. The field of view is  $30''$ ; North is up and East is to the left. *Right*— Zoomed-in version of the same image centered on the arc. The polygon is the aperture used to extract the arc photometry, while the smaller rectangle is the region within which the color was determined. The field of view is  $12''.5$  across. The images have been smoothed with 5 pixel and 3 pixel Gaussian kernels, respectively, to enhance the contrast.

at  $0.95\mu\text{m}$  and  $f < 3 \times 10^{-16} \text{ erg s}^{-1} \text{ cm}^{-2}$  at  $1.35\mu\text{m}$  ( $5\sigma$ ).<sup>8</sup> Given the non-detection of  $\text{Ly}\alpha$  with either GMOS or *HST*/WFC3 spectroscopy, *HST* narrow- or medium-band imaging may be the most promising avenue for refining the redshift estimate for this arc.

#### 4. CLUSTER MASS FROM STRONG LENSING

##### 4.1. Enclosed Mass within the Arc

Under the assumption of circular symmetry for the cluster lens, we calculate the total mass enclosed by the giant arc as a function of the source redshift. In this case the arc radius  $\theta_a$  ( $\sim 125 \text{ kpc}$  at  $z_L = 1.75$ ) identifies the radius of the tangential critical curve, which can be easily related to the enclosed mass through the relation,

$$M_a = \pi \Sigma_c \theta_a^2, \quad (1)$$

where  $\Sigma_c$  is the lensing surface critical density, which reads

$$\Sigma_c = \frac{c^2}{4\pi G} \frac{D_S}{D_L D_{LS}}. \quad (2)$$

In this equation  $D_L$ ,  $D_S$ , and  $D_{LS}$  are the angular diameter distances to the lens, to the source, and from the lens to the source, respectively.<sup>9</sup>

We emphasize that this enclosed mass is independent of the specific density profile assumed for the lens. One important caveat in this estimate, however, is that the assumption of circular symmetry is known to yield an overestimate of the enclosed mass for more realistic systems with intrinsic ellipticity. To approximately account for this effect, we assume that the circular model results in a factor of  $\sim 1.6$  overestimate of the mass, consistent with Bartelmann (1995), and quote values below that include this correction.

In Figure 2 we show the resulting enclosed mass as a function of the source redshift. The closer the source is to the deflector, the larger the enclosed mass needs to be due to the geometric suppression of the lensing efficiency. The uncertainty in the enclosed mass shown in the Figure corresponds

to the uncertainty in the arc radius, for which we adopt the nominal value of  $30 \text{ kpc}$  (see §2). The value for the enclosed mass reaches a lower limit of  $M_a = 6.9 \pm 0.3 \times 10^{13} M_\odot$  for  $z_s = 6$ . The enclosed mass in this central  $125 \text{ kpc}$  region, which contains minimal assumptions, already is comparable to the total mass inferred for the only spectroscopically confirmed cluster at higher redshift (Gobat et al. 2011).

##### 4.2. $M_{200}$

The next step is to estimate the total mass within  $r_{200}$  for the cluster. This problem is underconstrained, necessitating several simplifying assumptions. We initially assume that the density profile of the cluster is well represented by a spherical NFW model (Navarro et al. 1996, 1997). For a given virial mass, we compute the concentration of the dark matter halo according to the prescription of Gao et al. (2008), which is in turn a modified version of the original NFW prescription. The Gao et al. (2008) formula has been extensively tested against numerical simulations, including the high redshift regime relevant to the current analysis, and is expected to provide improvement over the prescriptions of Eke et al. (2001) and Bullock et al. (2001).

To account for asymmetries in the cluster mass distribution, we next assign a non-vanishing ellipticity to the lensing potential, according to the procedure summarized in Meneghetti et al. (2003). Finally, we assume that the arc is produced by a source lying near one of the caustic cusps situated along the major axis of the lens, so that the arc radius corresponds to the maximum elongation of the critical curve. Thus, we vary  $M_{200}$  until we find a match between this maximum elongation and  $\theta_a$ .

In Figure 2 we show the resulting  $M_{200}$  as a function of the source redshift. We assume an ellipticity,  $e_m \approx 0.32$ , consistent with the mean of the ellipticity distribution presented in Figure 7 of Fedeli & Berciano Alba (2009), and use the standard deviation of this distribution  $\sigma_e \approx 0.074$  to define the uncertainty shown by the shaded region. A caveat to this assumption is that this ellipticity distribution is derived at low redshift. Lee et al. (2005) however demonstrated that evolution of the ellipticity distribution is expected to be negligible for  $z < 1.5$ , and sufficiently small at  $z < 2$  as to not impact our calculations. From this analysis the derived value for  $M_{200}$  ap-

<sup>8</sup> <http://axe.stsci.edu/axesim/>

<sup>9</sup> We refer the reader to Meylan et al. (2006) for a detailed review of gravitational lensing.

proaches a lower limit of  $M_{200} = 2.8^{+1.0}_{-0.4} \times 10^{14} M_{\odot}$  as  $z_s \rightarrow 6$ , where the quoted uncertainty reflects the uncertainty in the ellipticity. For reference, we also show the results obtained with the same fiducial ellipticity  $e_m$ , but assuming the original NFW prescription for the concentration (dashed curve). Since at high redshift the NFW concentration is always higher than other prescriptions, the required  $M_{200}$  of the cluster is 35% smaller. Conversely, use of either the Bullock et al. (2001) or Eke et al. (2001) prescriptions would lead to a larger value of  $M_{200}$ .

It should be noted that strong cluster lenses are usually a biased subsample of the whole cluster population, in the sense that they tend to be intrinsically more concentrated, and to be prolated with the major axis aligned along the line of sight (Hennawi et al. 2007; Meneghetti et al. 2010). This bias is expected to be even more severe in redshift and/or mass ranges where strong lensing is particularly rare, such as the case under consideration. It has also recently been observed that there may be a stronger than expected correlation between concentration and cluster mass, with lower mass systems having higher than expected concentrations (e.g., Schmidt & Allen 2007; Etori et al. 2010; Oguri et al. 2012). Therefore, a concentration higher than that provided by the Gao et al. (2008) prescription, which is a mean over the entire cluster population, might actually be more realistic in this circumstance. As an example, for a sample of lensing clusters at  $z \sim 0.5$  Oguri et al. (2009) found concentrations a factor of  $\sim 2$  higher than would be predicted by the Gao et al. (2008) distribution. Simulations by Meneghetti et al. (2010) also indicate that projection effects may yield observed concentrations that are enhanced by up to a factor of two. In the current case, if we assume that the concentration is a factor of two above the Gao et al. (2008) prescription, then the derived  $M_{200}$  would decrease by roughly a factor of 2.2.

In Figure 2 and Table 1 we also present the masses and associated uncertainties derived from the Sunyaev-Zel'Dovich analysis (Brodwin et al. 2012). The two approaches appear to yield consistent estimates for  $M_{200}$  if the source redshift lies at  $z \gtrsim 3.5$ , or more conservatively  $z \gtrsim 3$  if one includes the potential for reducing the lensing mass by up to a factor of  $\sim 2$  if the halo concentration is larger than for a typical cluster. Coupled with the color of the arc, these factors together argue that the most plausible redshift is  $3 \lesssim z \lesssim 6$ .

## 5. COSMOLOGICAL IMPLICATIONS

The redshift of this cluster makes it a unique and interesting test for cosmological structure formation. To be specific, the most distant clusters known to host giant arcs prior to this study lie at  $z \sim 1$  (e.g., Gladders et al. 2003; Huang et al. 2009). IDCS J1426.5+3508 significantly extends the redshift baseline over which arcs are known to exist. In this section we consider the probability for this massive, strong lensing cluster to exist and be detected in our survey. Specifically, given a standard  $\Lambda$ CDM cosmology with the seven year WMAP cosmological parameters, what is the probability of detecting a giant arc of this brightness behind a cluster at  $z > 1.75$ ?

In order to estimate how rare the observed gravitational arc is, we evaluate the number of arcs in the whole sky that are expected to be produced by galaxy clusters at redshift larger than  $z_L = 1.75$ . We first estimate, for a fixed source redshift  $z_s$ , the contribution to the optical depth by structures in the desired redshift range,

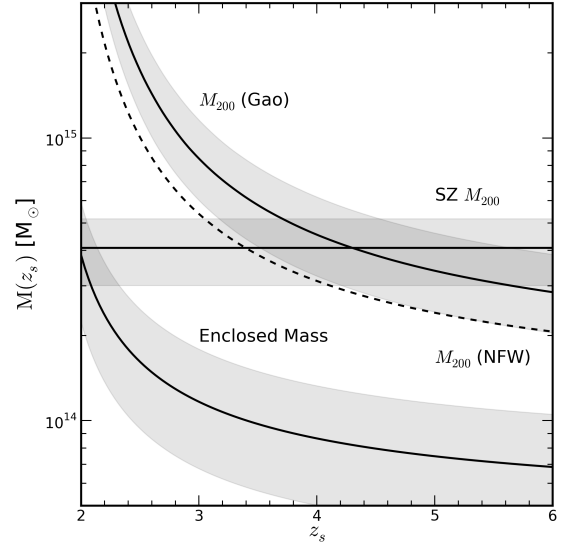


FIG. 2.— Mass of IDCS J1426.5+3508 as a function of redshift of the lensed source. The lower curve corresponds to the mass enclosed within the arc, with the shaded region denoting the uncertainty associated with the offset of the BCG relative to the cluster potential. The upper curve is the inferred  $M_{200}$  assuming the Gao et al. (2008) prescription for the concentration and an ellipticity  $e_m \approx 0.32$  for the cluster dark matter halo. In this case the uncertainty denoted by the shaded region is dominated by the intrinsic scatter in the distribution of halo ellipticities. We also overplot as a dashed line the inferred mass if one instead uses the original NFW prescription for the halo concentration (which can be considered a lower bound). The horizontal line and associated uncertainties correspond to the  $M_{200}$  derived from Sunyaev-Zel'dovich observations. In this case the uncertainties do not include the potential systematic bias associated with extrapolating SZ scaling relations to higher redshift.

$$\tau_q(z_s) = \frac{1}{4\pi D_S} \int_{z_L}^{z_s} dz \int_0^{+\infty} dM n(M, z) \left| \frac{dV(z)}{dz} \right| \sigma_q(M, z). \quad (3)$$

In the previous equation  $n(M, z)$  is the mass function of cosmic structures,  $dV(z)/dz$  represents the comoving volume of space per unit redshift, and  $\sigma_q(M, z)$  stands for the cross section of individual clusters for images having the morphological property  $q$ . In what follows we assume that  $q$  is a length-to-width ratio  $\geq 10$ , as customary in arc statistics studies, and employ the Tinker et al. (2008) mass function.

The total number of arcs with the property  $q$  that are observed in the sky with a magnitude brighter than  $m$  then simply reads

$$N_q(m) = 4\pi n_S(m) \int_{z_L}^{+\infty} p(z_s, m) \tau_q(z_s) dz_s, \quad (4)$$

where  $p(z_s, m)$  is the source redshift distribution, while  $n_S(m)$  represents the observed number density of sources with magnitude lower than  $m$ , i.e., the cumulative number counts. We adopt the redshift distribution and number counts for sources in the *Hubble* UDF provided by Coe et al. (2006) for F775W and F160W, and correct the number counts for the lensing magnification bias using the same procedure detailed in Fedeli et al. (2008) and Fedeli & Berciano Alba (2009).

For the practical computation of the optical depth, we use the strategy detailed in Fedeli et al. (2008) and references therein. Briefly, merger trees are constructed based on the extended Press & Schechter (1974) theory, which represent a

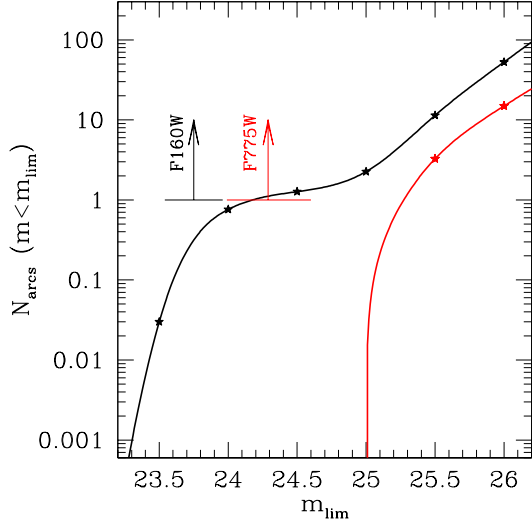


FIG. 3.— Predicted number of giant arcs over the entire sky as a function of magnitude in F775W and F160W for clusters at  $z > 1.75$ . The points correspond to the results from our simulations, while the curves are spline interpolations between the data points. The arrows represent the all-sky lower limits derived from the observed arc in IDCS J1426.5+3508, with the width at the bottom of the arrows corresponding to the photometric uncertainty. We note that finding one arc per  $8.82 \text{ deg}^2$  would correspond to  $\sim 4700$  arcs all-sky.

model of the cluster population. A lensing potential ellipticity is assigned to each cluster, extracted from the distribution shown in Fedeli & Berciano Alba (2009), and cluster dynamical activity occurring at the knots of the merger trees is suitably modeled. Individual clusters are modeled as NFW profiles with the assigned potential ellipticity, and the concentration is linked to the mass through the Gao et al. (2008) prescription for the concentration, consistent with §4.2. We include a lognormal scatter in the concentration with  $\sigma_c = 0.2$ , as in Fedeli et al. (2007). Finally, the cluster cross sections for giant arcs are computed using the fast and semi-analytic prescription of Fedeli et al. (2006), and the optical depth integrals are approximated by using a Monte-Carlo scheme.

Figure 3 shows the resulting number of arcs expected across the full sky as a function of magnitude in F775W and F160W. For our observed arc we assume a color correction  $F775W - F814W \approx 0.0$  (AB), consistent with the expected color of a star-forming galaxy at this epoch. For the observed magnitudes we expect to find **no** arcs over the entire sky as bright in F814W as the one we observe and only  $\sim 0.3$  as bright in F160W. Indeed, none are expected within 0.5 magnitudes of the brightness of the arc in F814W. Given that the area of our survey is only  $8.82 \text{ deg}^2$  ( $2 \times 10^{-4}$  of the full sky), the detection of an arc is highly implausible. For reference, we test the sensitivity of this result to the redshift of the lensing cluster. Even if one were to consider the entire cluster population at  $z > 1.5$  rather than setting the observed cluster redshift as the minimum permitted redshift, then the expected number of arcs detected remains zero in F814W and  $\sim 15$  all-sky in F160W. The latter still leaves only a probability of  $2 \times 10^{-3}$  that we would have detected such an arc in this survey. Note that the specific mass of IDCS J1426.5+3508 does not enter into our calculations – we posed the question of how many arcs should be produced by *all* clusters.

At lower redshifts the excess of giant arcs behind clus-

ters relative to predictions has been realized for well over a decade (e.g., Bartelmann et al. 1998) and is known as the arc statistics problem. While significant effort has been devoted to reconcile the observations with improved models that incorporate more detailed physics and improved constraints on the source redshift distribution (e.g., Bartelmann et al. 2003; Wambsganss et al. 2004; Dalal et al. 2004; Li et al. 2006; Fedeli et al. 2008; Wambsganss et al. 2008; D’Aloisio & Natarajan 2011), the issue is not wholly resolved (e.g., Meneghetti et al. 2011). The current cluster greatly exacerbates the situation – this arc simply *should not exist*.

It is interesting to break down the above calculation of the number of arcs (Equation 4) to ascertain the dominant factor that drives the expected number of arcs to zero. The two fundamental physical quantities that determine the total number of arcs are the total lensing optical depth of all clusters and the number density of background sources to be lensed.

The lensing optical depth depends upon the products of the cluster mass function and the lensing efficiency of individual clusters, which is a strong function of cluster mass. An obvious explanation would be if IDCS J1426.5+3508 exceeds the mass of clusters expected to exist in a  $\Lambda$ CDM universe at this redshift. If lensing requires reaching a critical mass threshold that is exceeded in reality but not in our model, then the observed number of arcs would clearly exceed expectations. In that case, a plausible solution would be to invoke non-Gaussianity to enhance the number of extremely massive clusters. It is however argued in Brodwin et al. (2012) that IDCS J1426.5+3508 is consistent with  $\Lambda$ CDM, indicating that invoking non-Gaussianity is not necessarily the appropriate solution.

A more subtle solution would be if the lensing cross-sections of individual clusters systematically exceed the calculated theoretical cross-sections. There is evidence that this lensing efficiency is indeed systematically underestimated. Several papers have argued that including the impact of baryonic contraction can raise the lensing cross-section by between 25% and a factor of two (Li et al. 2006; Wambsganss et al. 2008). Meneghetti et al. (2011) also find that simulated clusters produce  $\sim 50\%$  fewer arcs than X-ray clusters at  $z \approx 0.5 - 0.7$ . While these corrections work in the proper direction, it appears that even if one imposes reasonable physical tweaks to account for the impact of baryonic infall on the density profile, the change remains insufficient to account for the arc in IDCS J1426.5+3508. Moreover, as demonstrated by Mead et al. (2010), inclusion of AGN feedback acts to counteract the impact of baryonic infall, resulting in a smaller enhancement to the cross-section. Even ignoring the mitigating effect of feedback, the discrepancy is simply too large. Specifically, doubling the predicted number of arcs would imply  $\sim 1$  arc *all-sky* with the observed F160W magnitude, and would still imply none with the observed F775W magnitude.

Another means of boosting the effective cross-section for an individual system is via the presence of additional structures along the line of sight. Puchwein & Hilbert (2009) used the Millenium simulations to quantify the impact of such secondary structures. These authors found that the typical impact is to enhance the cross section by 10 – 25%, with enhancements of 50% not uncommon for individual systems. Again, this factor alone is insufficient to explain the discrepancy.

The final factor that can drive the prediction of zero arcs is underestimation of the surface density of galaxies sufficiently



TABLE 1. DERIVED MASSES FOR IDCS J1426.5+3508

| Method  | Radius    | Mass ( $10^{14} M_{\odot}$ ) |
|---------|-----------|------------------------------|
| Lensing | 125 kpc   | $> 0.69 \pm 0.03$            |
| Lensing | $r_{200}$ | $> 2.8^{+1.0}_{-0.4}$        |
| SZ      | $r_{500}$ | $2.6 \pm 0.7$                |
| SZ      | $r_{200}$ | $4.1 \pm 1.1$                |

NOTE. — The lensing limiting masses correspond to the maximum possible source redshift,  $z_s = 6$ . Both  $M_{200}$  masses presume a concentration consistent with the Gao et al. (2008) relation. If the projected concentration is a factor of two higher then the lensing and SZ masses drop by factors of 2.1 and 1.2, respectively. As noted in the text,  $r_{500}$  and  $r_{200}$  are defined relative to critical density.

bright to yield a source similar to the observed arc after magnification by the cluster potential. One concern here is that we have used results from the UDF to inform our redshift distribution for background sources, yet this region is sufficiently small that cosmic variance is a concern. As an alternate test, we also try an analytic prescription for the background number counts based upon the  $z \sim 3$  luminosity function of Reddy et al. (2008) to model the background distribution. We find however that this approach does not qualitatively alter the results of our analysis. It therefore seems unlikely that error in the source distribution is the origin of the discrepancy.

We therefore identify no obvious physical solution to explain the existence of this arc, though exceptionally high concentrations seems like the most promising avenue to explore. Finally, a last possible solution would be if the observed source is not a background arc. Given the combination of color, curvature,  $l/w$ , and lack of color variation, this possibility also seems unlikely.

## 6. CONCLUSIONS

We have presented evidence for the existence of a giant arc behind the massive galaxy cluster IDCS J1426.5+3508 at  $z = 1.75$ . This unique system constitutes the highest redshift cluster known to host a giant arc. From the strong lensing we derive an enclosed lensing mass within the central 125 kpc of  $M_a > 6.9 \pm 0.3 \times 10^{13} M_{\odot}$ , which is comparable to (or exceeds) the *total* masses of most other known clusters at  $z > 1.5$ , confirming that IDCS J1426.5+3508 is an exceptionally massive cluster at this epoch. Having derived the enclosed mass, we next provide a comparison with the Sunyaev-Zel'Dovich-derived value of  $M_{200}$  from Brodwin et al. (2012). We find that the two are consistent if the arc lies at  $z \gtrsim 3$ , and derive a lower bound on the mass of  $M_{200} > 2.8 \times 10^{14} M_{\odot}$ .

Finally, we investigate the cosmological implications of this system. The greatest challenge posed by this cluster is explaining the existence of the giant arc at all. In §5 we demonstrate that under realistic assumptions for the lensing cross-section, cluster mass function, and background galaxy distribution, the total number of giant arcs behind clusters at

$z > 1.75$  that are at least as bright as the observed arc is zero in F814W and  $< 1$  in F160W. Very simply, the arc we have discovered behind IDCS J1426.5+3508 is not predicted to exist. If one considers an ensemble of lensing clusters extending to somewhat lower redshift,  $z > 1.5$ , the tension with theoretical expectations decreases slightly for F160W, but in F814W the number of predicted arcs remains zero. We briefly discuss possible explanations for this discrepancy, but find no obvious solution. A tendency of higher concentrations in observed clusters than simulated systems has the greatest potential to decrease the disparity, but is unlikely to be sufficient to reconcile theoretical models for arc statistics with the existence of a lensing cluster at  $z = 1.75$ .

Looking towards the future, a statistical sample of the most massive clusters in the Universe at  $z = 1 - 2$  will provide the means with which to ascertain the true frequency of arcs behind high-redshift clusters. Much as the frequency of strong lensing clusters at  $z = 0.5 - 1$  was a surprise a decade ago, it appears that this higher redshift regime is poised to yield further unexpected discoveries.

The authors thank the anonymous referee for suggestions that improved the quality of this paper. We are also grateful to Gemini Observatory for allocating Director's Discretionary time to obtain a redshift for the giant arc. We appreciate the support provided by Nancy Levenson and the rest of the Gemini staff for this project. Gemini Observatory is operated by the Association of Universities for Research in Astronomy, Inc., under a cooperative agreement with the NSF on behalf of the Gemini partnership: the National Science Foundation (United States), the Science and Technology Facilities Council (United Kingdom), the National Research Council (Canada), CONICYT (Chile), the Australian Research Council (Australia), Ministério da Ciência, Tecnologia e Inovação (Brazil) and Ministerio de Ciencia, Tecnología e Innovación Productiva (Argentina). This work is based in part on data obtained at the W. M. Keck Observatory, which is operated as a scientific partnership among the California Institute of Technology, the University of California and the National Aeronautics and Space Administration. Support for this research was provided by NASA through HST GO programs 11663 and 12203. AHG thanks Marusa Bradáč for a useful discussion about the arc, and also acknowledges support from the National Science Foundation through grant AST-0708490. The work by SAS at LLNL was performed under the auspices of the U. S. Department of Energy under Contract No. W-7405-ENG-48, and support for MB was provided by the W. M. Keck Foundation. The work of PRME and DS was carried out at Jet Propulsion Laboratory, California Institute of Technology, under a contract with NASA. The research activities of AD are supported by NOAO, which is operated by the Association of Universities for Research in Astronomy (AURA) under a cooperative agreement with the National Science Foundation.

## REFERENCES

- Ashby, M. L. N., Stern, D., Brodwin, M., Griffith, R., Eisenhardt, P., Kozłowski, S., Kochanek, C. S., Bock, J. J., Borys, C., Brand, K., Brown, M. J. I., Cool, R., Cooray, A., Croft, S., Dey, A., Eisenstein, D., Gonzalez, A. H., Gorjian, V., Grogin, N. A., Ivison, R. J., Jacob, J., Jannuzi, B. T., Mainzer, A., Moustakas, L. A., Röttgering, H. J. A., Seymour, N., Smith, H. A., Stanford, S. A., Stauffer, J. R., Sullivan, I., van Breugel, W., Willner, S. P., & Wright, E. L. 2009, *ApJ*, 701, 428
- Bartelmann, M. 1995, *A&A*, 299, 11
- Bartelmann, M., Huss, A., Colberg, J. M., Jenkins, A., & Pearce, F. R. 1998, *A&A*, 330, 1
- Bartelmann, M., Meneghetti, M., Perrotta, F., Baccigalupi, C., & Moscardini, L. 2003, *A&A*, 409, 449
- Bertin, E. & Arnouts, S. 1996, *A&AS*, 117, 393
- Brodwin, M., Gonzalez, A. H., Stanford, S. A., Stern, D., Dey, A., Zeimann, G., Eisenhardt, P. R., Mancone, C., Plagge, T., & Carlstrom, J. 2012, *ApJ*
- Bruzual, G. & Charlot, S. 2003, *MNRAS*, 344, 1000

- Bullock, J. S., Kolatt, T. S., Sigad, Y., Somerville, R. S., Kravtsov, A. V., Klypin, A. A., Primack, J. R., & Dekel, A. 2001, *MNRAS*, 321, 559
- Carlberg, R. G., Yee, H. K. C., Ellingson, E., Abraham, R., Gravel, P., Morris, S., & Pritchet, C. J. 1996, *ApJ*, 462, 32
- Cayón, L., Gordon, C., & Silk, J. 2011, *MNRAS*, 415, 849
- Chabrier, G. 2003, *PASP*, 115, 763
- Coe, D., Benítez, N., Sánchez, S. F., Jee, M., Bouwens, R., & Ford, H. 2006, *AJ*, 132, 926
- Dalal, N., Holder, G., & Hennawi, J. F. 2004, *ApJ*, 609, 50
- D'Aloisio, A. & Natarajan, P. 2011, *MNRAS*, 415, 1913
- Donahue, M., Voit, G. M., Gioia, I., Lupino, G., Hughes, J. P., & Stocke, J. T. 1998, *ApJ*, 502, 550
- Eke, V. R., Navarro, J. F., & Steinmetz, M. 2001, *ApJ*, 554, 114
- Enqvist, K., Hotchkiss, S., & Taanila, O. 2011, *JCAP*, 4, 17
- Ettori, S., Gastaldello, F., Leccardi, A., Molendi, S., Rossetti, M., Buote, D., & Meneghetti, M. 2010, *A&A*, 524, A68
- Fedeli, C., Bartelmann, M., Meneghetti, M., & Moscardini, L. 2007, *A&A*, 473, 715
- . 2008, *A&A*, 486, 35
- Fedeli, C. & Berciano Alba, A. 2009, *A&A*, 508, 141
- Fedeli, C., Meneghetti, M., Bartelmann, M., Dolag, K., & Moscardini, L. 2006, *A&A*, 447, 419
- Ford, H. C., Clampin, M., Hartig, G. F., Illingworth, G. D., Sirianni, M., Martel, A. R., Meurer, G. R., McCann, W. J., Sullivan, P. C., Bartko, F., Benítez, N., Blakeslee, J., Bouwens, R., Broadhurst, T., Brown, R. A., Burrows, C. J., Campbell, D., Cheng, E. S., Feldman, P. D., Franx, M., Golimowski, D. A., Gronwall, C., Kimble, R. A., Krist, J. E., Lesser, M. P., Magee, D., Miley, G., Postman, M., Rafal, M. D., Rosati, P., Sparks, W. B., Tran, H. D., Tsvetanov, Z. I., Volmer, P., White, R. L., & Woodruff, R. A. 2003, in Presented at the Society of Photo-Optical Instrumentation Engineers (SPIE) Conference, Vol. 4854, Future EUV/UV and Visible Space Astrophysics Missions and Instrumentation. Edited by J. Chris Blades, Oswald H. W. Siegmund. Proceedings of the SPIE, Volume 4854, pp. 81-94 (2003), ed. J. C. Blades & O. H. W. Siegmund, 81-94
- Gao, L., Navarro, J. F., Cole, S., Frenk, C. S., White, S. D. M., Springel, V., Jenkins, A., & Neto, A. F. 2008, *MNRAS*, 387, 536
- Gladders, M. D., Hoekstra, H., Yee, H. K. C., Hall, P. B., & Barrientos, L. F. 2003, *ApJ*, 593, 48
- Gobat, R., Daddi, E., Onodera, M., Finoguenov, A., Renzini, A., Arimoto, N., Bouwens, R., Brusa, M., Chary, R.-R., Cimatti, A., Dickinson, M., Kong, X., & Mignoli, M. 2011, *A&A*, 526, A133+
- Gonzalez, V., Bouwens, R., Labbe, I., Illingworth, G., Oesch, P., Franx, M., & Magee, D. 2011, *ArXiv e-prints*
- Hennawi, J. F., Dalal, N., Bode, P., & Ostriker, J. P. 2007, *ApJ*, 654, 714
- Hoyle, B., Jimenez, R., & Verde, L. 2011, *Phys. Rev. D*, 83, 103502
- Huang, X., Morokuma, T., Fakhouri, H. K., Aldering, G., Amanullah, R., Barbary, K., Brodwin, M., Connolly, N. V., Dawson, K. S., Doi, M., Faccioli, L., Fadeyev, V., Fruchter, A. S., Goldhaber, G., Gladders, M. D., Hennawi, J. F., Ihara, Y., Jee, M. J., Kowalski, M., Konishi, K., Lidman, C., Meyers, J., Moustakas, L. A., Perlmutter, S., Rubin, D., Schlegel, D. J., Spadafora, A. L., Suzuki, N., Takanashi, N., & Yasuda, N. 2009, *ApJ*, 707, L12
- Kimble, R. A., MacKenty, J. W., O'Connell, R. W., & Townsend, J. A. 2008, in Presented at the Society of Photo-Optical Instrumentation Engineers (SPIE) Conference, Vol. 7010, Society of Photo-Optical Instrumentation Engineers (SPIE) Conference Series
- Komatsu, E., Smith, K. M., Dunkley, J., Bennett, C. L., Gold, B., Hinshaw, G., Jarosik, N., Larson, D., Nolta, M. R., Page, L., Spergel, D. N., Halpern, M., Hill, R. S., Kogut, A., Limon, M., Meyer, S. S., Odegard, N., Tucker, G. S., Weiland, J. L., Wollack, E., & Wright, E. L. 2011, *ApJS*, 192, 18
- Lee, J., Jing, Y. P., & Suto, Y. 2005, *ApJ*, 632, 706
- Li, G. L., Mao, S., Jing, Y. P., Mo, H. J., Gao, L., & Lin, W. P. 2006, *MNRAS*, 372, L73
- Mead, J. M. G., King, L. J., Sijacki, D., Leonard, A., Puchwein, E., & McCarthy, I. G. 2010, *MNRAS*, 406, 434
- Meneghetti, M., Bartelmann, M., & Moscardini, L. 2003, *MNRAS*, 340, 105
- Meneghetti, M., Fedeli, C., Pace, F., Gottlöber, S., & Yepes, G. 2010, *A&A*, 519, A90+
- Meneghetti, M., Fedeli, C., Zitrin, A., Bartelmann, M., Broadhurst, T., Gottlöber, S., Moscardini, L., & Yepes, G. 2011, *A&A*, 530, A17
- Meylan, G., Jetzer, P., North, P., Schneider, P., Kochanek, C. S., & Wambsganss, J., eds. 2006, *Gravitational Lensing: Strong, Weak and Micro*, ed. G. Meylan, P. Jetzer, P. North, P. Schneider, C. S. Kochanek, & J. Wambsganss
- Mullis, C. R., Rosati, P., Lamer, G., Böhringer, H., Schwöpe, A., Schuecker, P., & Fassbender, R. 2005, *ApJ*, 623, L85
- Navarro, J. F., Frenk, C. S., & White, S. D. M. 1996, *ApJ*, 462, 563
- . 1997, *ApJ*, 490, 493
- Oguri, M., Bayliss, M. B., Dahle, H., Sharon, K., Gladders, M. D., Natarajan, P., Hennawi, J. F., & Koester, B. P. 2012, *MNRAS*, 2189
- Oguri, M., Hennawi, J. F., Gladders, M. D., Dahle, H., Natarajan, P., Dalal, N., Koester, B. P., Sharon, K., & Bayliss, M. 2009, *ApJ*, 699, 1038
- Press, W. H. & Schechter, P. 1974, *ApJ*, 187, 425
- Puchwein, E. & Hilbert, S. 2009, *MNRAS*, 398, 1298
- Reddy, N. A., Steidel, C. C., Pettini, M., Adelberger, K. L., Shapley, A. E., Erb, D. K., & Dickinson, M. 2008, *ApJS*, 175, 48
- Rosati, P., Tozzi, P., Gobat, R., Santos, J. S., Nonino, M., Demarco, R., Lidman, C., Mullis, C. R., Strazzullo, V., Böhringer, H., Fassbender, R., Dawson, K., Tanaka, M., Jee, J., Ford, H., Lamer, G., & Schwöpe, A. 2009, *A&A*, 508, 583
- Sanderson, A. J. R., Edge, A. C., & Smith, G. P. 2009, *MNRAS*, 398, 1698
- Schmidt, R. W. & Allen, S. W. 2007, *MNRAS*, 379, 209
- Stanford, S. A., Brodwin, M., Gonzalez, A. H., Stern, D., Dey, A., Zeimann, G., Eisenhardt, P. R., & Mancone, C. 2012, *ApJ*, 000, 000
- Tinker, J., Kravtsov, A. V., Klypin, A., Abazajian, K., Warren, M., Yepes, G., Gottlöber, S., & Holz, D. E. 2008, *ApJ*, 688, 709
- Wambsganss, J., Bode, P., & Ostriker, J. P. 2004, *ApJ*, 606, L93
- Wambsganss, J., Ostriker, J. P., & Bode, P. 2008, *ApJ*, 676, 753
- Williamson, R., Benson, B. A., High, F. W., Vanderlinde, K., Ade, P. A. R., Aird, K. A., Andersson, K., Armstrong, R., Ashby, M. L. N., Bautz, M., Bazin, G., Bertin, E., Bleem, L. E., Bonamente, M., Brodwin, M., Carlstrom, J. E., Chang, C. L., Chapman, S. C., Clocchiatti, A., Crawford, T. M., Crites, A. T., de Haan, T., Desai, S., Dobbs, M. A., Dudley, J. P., Fazio, G. G., Foley, R. J., Forman, W. R., Garmire, G., George, E. M., Gladders, M. D., Gonzalez, A. H., Halverson, N. W., Holder, G. P., Holzappel, W. L., Hoover, S., Hrubes, J. D., Jones, C., Joy, M., Keisler, R., Knox, L., Lee, A. T., Leitch, E. M., Lueker, M., Luong-Van, D., Marrone, D. P., McMahon, J. J., Mehl, J., Meyer, S. S., Mohr, J. J., Montroy, T. E., Murray, S. S., Padin, S., Plagge, T., Pryke, C., Reichardt, C. L., Rest, A., Ruel, J., Ruhl, J. E., Saliwanchik, B. R., Saro, A., Schaffer, K. K., Shaw, L., Shirokoff, E., Song, J., Spieler, H. G., Stalder, B., Stanford, S. A., Staniszewski, Z., Stark, A. A., Story, K., Stubbs, C. W., Vieira, J. D., Vikhlinin, A., & Zenteno, A. 2011, *ApJ*, 738, 139
- Wu, X.-P. & Hammer, F. 1993, *MNRAS*, 262, 187
- Zwicky, F. 1933, *Helvetica Physica Acta*, 6, 110